Structural Chemistry (2019) 30:2159–2166
https://doi.org/10.1007/s11224-019-01354-5

ORIGINAL RESEARCH

The conformation of biliverdin in dimethyl sulfoxide: implications for the coordination with copper

Milena S. Dimitrijević[1] · Milan Žižić[1] · Mario Piccioli[2] · Jelena Bogdanović Pristov[1] · Ivan Spasojević[1]

Received: 1 April 2019 / Accepted: 7 May 2019 / Published online: 20 May 2019

Abstract

Biliverdin (BV) structure was analyzed by using NMR techniques and unrestricted density function theory simulations to explain the incapacity of BV to build coordination complex(es) with Cu^{2+} in dimethyl sulfoxide, which was confirmed by UV-Vis, EPR and NMR spectroscopy. NMR showed that N atoms are protonated in all four pyrrole rings. The structure is stabilized by two hydrogen bonds between NH moieties and carbonyl oxygens from opposite terminal pyrrole rings, and by the bending of propionyl chain with carboxyl group out of the plain toward central position of BV. The simulations of deprotonated BV, which builds copper complexes in water and chloroform as described previously, showed a different conformation and organization of hydrogen bonds. Taking into account that deprotonation represents a critical step in coordinate bonds formation, the protonation of an additional N atom may represent a key difference between the interactions of BV with copper in different solvents.

Keywords Biliverdin · Copper · Hydrogen bonds · NOESY · UDFT

Introduction

The change of solvent may be a dramatic event for some molecules [1]. Solvents may affect protonation, hydrogen bonding, conformation and, as a result, physico-chemical properties, and biochemical/pharmacological performance, such as in the case of solvent-induced isomerization and molecular switching of tetrapyrroles [2, 3]. Biliverdin (BV) is a naturally occurring tetrapyrrolic bile pigment with two propionic acid side chains. BV is produced by degradation of heme-iron protoporphyrin IX complex, and it is further reduced to bilirubin by biliverdin reductase [4, 5]. In aqueous media, BV has two deprotonated carboxyl groups (*pKa* values at 3.9 and 5.3), and tends to acquire a distorted helical conformation that is stabilized mainly by intramolecular hydrogen bonding between unprotonated and protonated N atoms in pyrroles [6–9]. On the other hand, BV is usually solvated in dimethyl sulfoxide (DMSO), an aprotic polar solvent [10], for the purposes of stock preparation, extraction, and coordination complexes synthesis [11–13]. It has been shown that the interaction of DMSO with bile pigments and other porphyrins may be as follows: (i) affect *pK* values of carboxyl groups [14–17], (ii) interfere with hydrogen bonds [8, 18, 19], and (iii) change redox properties [10, 20]. Importantly, different solvents may impact on the interactions of BV and related compounds with transition metals [5, 21]. It has been shown that a BV analog and Cu^{2+} in chloroform build a ferromagnetically coupled $S = 1$ Cu^{2+}/BV radical cation system or a $S = 1$ Cu^{3+} BV trianion system [22]. On the other hand, we have shown recently that BV and Cu^{2+} in phosphate buffer form an $S = 0$ complex that is composed of either Cu^{1+} and BV radical cation or Cu^{3+} and BV radical anion [5]. Finally, it has been proposed that BV cannot form a complex with Cu^{2+} in DMSO and in aqueous solutions with low pH, most likely because Cu^{2+} cannot replace the NH protons [12].

Herein, we applied ^{1}H NMR spectroscopy and unrestricted density function theory (UFDT) simulations to elucidate the protonation and conformation of BV in DMSO, and to explain the lack of capacity of BV to build Cu complex(es) in this solvent.

Electronic supplementary material The online version of this article (https://doi.org/10.1007/s11224-019-01354-5) contains supplementary material, which is available to authorized users.

✉ Milan Žižić
mzizic1004@gmail.com

✉ Ivan Spasojević
redoxsci@gmail.com

[1] Department of Life Sciences, Institute for Multidisciplinary Research, University of Belgrade Kneza Višeslava 1, Belgrade 11030, Serbia

[2] Center for Magnetic Resonance, University of Florence, Via L. Sacconi 6, Sesto Fiorentino, 50019 Florence, Italy

Experimental

Chemicals

BV · HCl (purity ≥ 97%), $CuCl_2$, DMSO, and DMSO-d_6 (deuterated DMSO, 99.9% D atom) were purchased from Merck (Kenilworth, NJ, USA). Special care was taken to protect DMSO from atmospheric water. All experiments and stocks (BV (20 mM) and Cu^{2+} (100 mM)) were prepared in DMSO.

NMR spectroscopy

NMR experiments were recorded on a Bruker Avance 500 spectrometer, equipped with 5 mm cryoprobes. 1D experiments were collected with 64 scans, using 1.1 s and 3.0 s as acquisition and recycle delays, respectively. Residual DMSO signal was suppressed using selective saturation during the recycle delay. A 1-Hz exponential multiplication was applied to free induction decay (FID) signals prior to Fourier Transformation. NOESY experiment was performed using a 2048 × 440 data point matrix. Sixteen scans were collected for each FID; 90 ms, 300 ms, and 4 s were used as acquisition, mixing, and recycle delays, respectively. TOCSY experiment was acquired using a 2048 × 512 data point matrix, with eight scans each fid and using a 8-kHz spin lock field. 90 ms, 80 ms, and 4 s were used as acquisition, mixing, and recycle delays, respectively. Natural abundance ^{13}C-^{1}H HSQC spectrum was acquired with 48 scans for each FID, using a 2048 × 220 data point matrix. All the 2D experiments were processed by applying squared cosine bell weighting functions in both dimensions prior to Fourier transformation.

UDFT simulations

The optimizations of geometry of BV with four or three protonated N atoms - BVH^+ and BV in their ground states were performed using UDFT with M06-2X density functional and 6-31G(d) basis set, starting from closed ring conformations. To account for solvent effects, all computations were performed using the polarized continuum model and DMSO as a solvent. The absence of computed imaginary frequencies confirmed that the optimized structures corresponded to relative minima on potential energy surfaces. All simulations were performed with Gaussian 09 (Rev. D.01) program suite (Gaussian, Inc. Wallingford, CT, USA).

UV-Vis spectroscopy

UV-Vis spectra were recorded for BV and BV/Cu^{2+} = 1 system in DMSO during the period of 12 h, using a Jenway Genova Plus Spectrophotometer (Staffordshire, UK). Samples were freshly prepared and scanned at wavelengths from 250 to 950 nm with a scan interval of 2 nm at room temperature. Each scan was performed on a 1-mL aliquote of the sample to prevent potential effects of photodegradation.

EPR spectroscopy

Low-T EPR spectra of Cu^{2+} were recorded on a Bruker Elexsys II E540 spectrometer operating at X-band (9.4 GHz), using the Bruker N_2 Temperature Controller ER4131VT to maintain T at 110 K. The experimental parameters were as follows: microwave power, 3.17 mW; scan time, 80 s; modulation amplitude, 0.5 mT; modulation frequency, 100 kHz; and number of accumulations, 4. Samples were placed in quartz cuvettes (Wilmad-LabGlass, Vineland, NJ, USA), and frozen in cold isopentane after 5 min incubation period. Concentrations of copper and BV were 40 μM.

Results and discussion

Biliverdin structure—NMR

This is the first study presenting a detailed assignment of ^{1}H NMR signals of BV in DMSO (Fig. 1; Table 1). The assignment was performed by 2D NMR techniques—^{13}C-^{1}H HSQC, ^{1}H-^{1}H TOCSY (presented in Electronic supplementary material Fig. S1; Table 2), and ^{1}H-^{1}H NOESY, and by comparison to previous work on BV in other solvents and on bilirubin in DMSO [23, 24]. The broad, downfielded signal at 12.29 ppm was assigned to the two protons of propionyl carboxyl groups (H8). The two pairs of singlets at 11.98 and 11.90, and at 10.75 and 10.64 ppm were assigned to amino protons in inner (C and B) pyrrole rings, and in terminal (A and D) pyrrole rings, respectively. The difference in δ was larger for A and D (0.11 ppm) than C and B (0.08 ppm). Signal at 7.58 ppm is from methyne proton—H5, which is not present in bilirubin structure (and in its ^{1}H NMR spectrum) [25]. The assignment was confirmed by ^{13}C-^{1}H HSQC showing that H5 is positioned on C atom with δ = 119.36 ppm, a chemical shift that has been related to methyne group [26]. The intensity of H5 peak was further used as a reference integral intensity for one proton. The comparison of intensities showed that H8 signal comes from two protons, while peaks A-D arise from one proton each. This means that both carboxyl groups and all four N atoms are protonated in BV in DMSO. The pH value of BV solution in DMSO was around 4, i.e., below or near *pKa* values for carboxyl groups in BV that have been previously determined in water [7]. In addition, it has been shown that DMSO affects *pKa* values of propionic acid side chains [16, 17]. Theory suggests that the *pKa* should be inversely proportional to the dielectric constant of the medium (ε_r = 46.7 for DMSO, and ε_r = 80.1 for water) [27]. In line with this, a steep rise of *pKa* value for carboxyl groups has been observed to

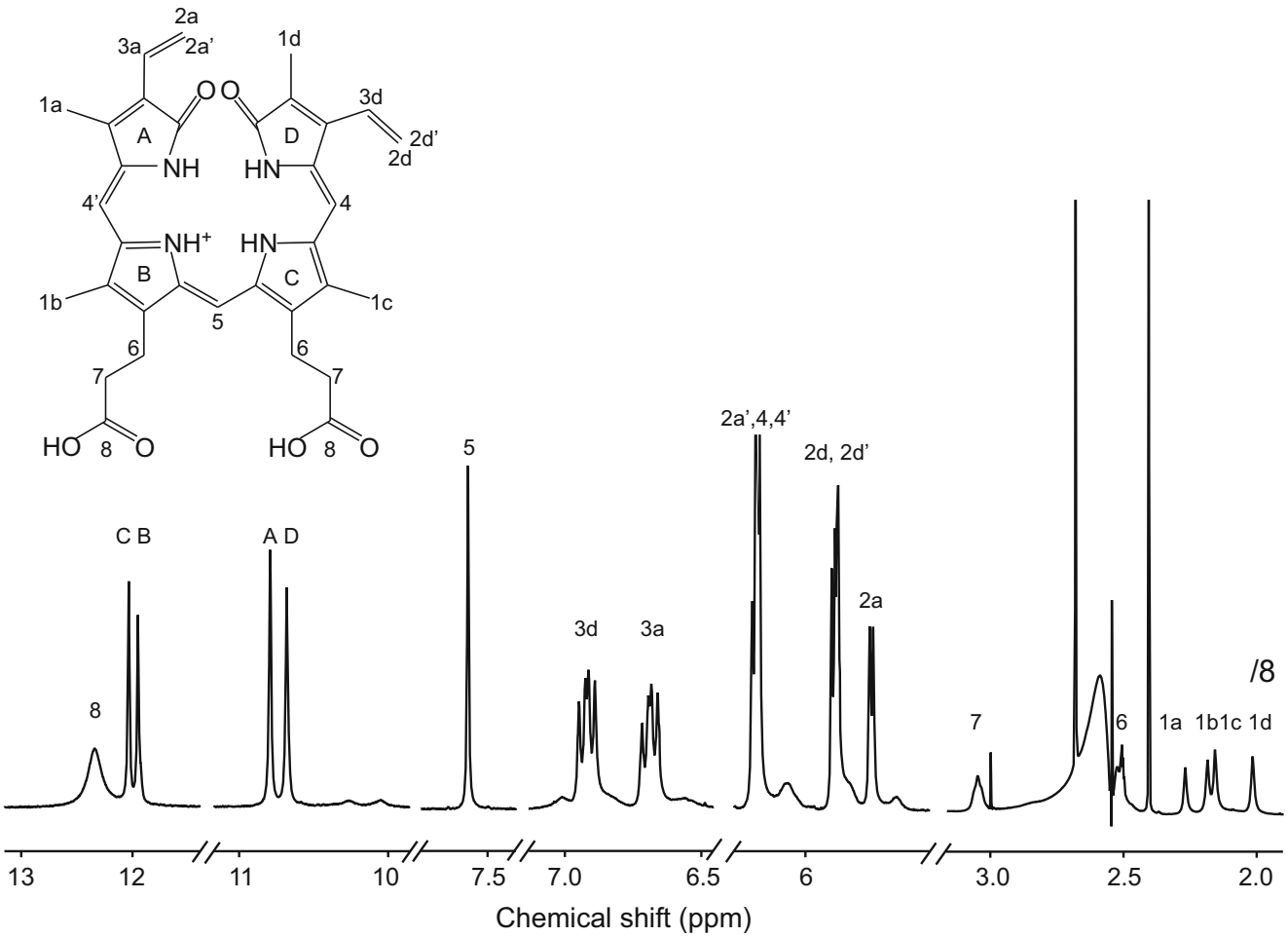

Fig. 1 ^{1}H NMR spectra of biliverdin in DMSO at 500 MHz and 298 K. The pH of the solution ([BV] = 2 mM) was ~ 4. The vertical intensity of the 3–2 ppm region is divided by a factor 8

take place with increasing fraction of DMSO in water-DMSO mixture [16]. Further, BV showed protonation of an additional N atom/pyrrole (and one positive charge) in DMSO, compared to three NH groups in BV in water solution [7, 8]. The extra proton came from HCl which is present in BV preparation. This is also suggested by the pH value of a 2 mM BV · HCl (pH = 4) compared to the pH of a 2 mM HCl (pH = 3.4); i.e., the higher pH of BV HCl solution compared to equimolar HCl implies that there are less free H^{+} in the first solution since they are bound to BV.

The next two signals at 6.91 ppm and 6.69 ppm represent doublets of doublets, which identified these signals as CH protons from pyrrole D and pyrrole A—H3d and H3a, which are coupled with non-equivalent methylene protons from the vinyl groups (refer to structure in Fig. 1). NOESY spectrum showed that H3d is close to H4 (Fig. 2), which is possible only for pyrrole D. The intensities of signals at 6.35, 6.32, and 6.31 ppm, and at 5.83, 5.81, 5.79, and 5.78 ppm, correspond to three and two protons, respectively. It is important to note that H4 and H4' atoms in two methyne bridges show different shifts (6.32 and 6.31 ppm). ^{13}C -^{1}H HSQC spectrum shows that the peak at 6.35 ppm, together with a doublet at 5.58 ppm, correlate with ^{13}C resonance at 122.10 ppm. This indicates that there are two diastereomeric protons from the CH_2 group. The HSQC experiment also showed a correlation in the region ca. 6.31/95 ppm; a close-up of the peak indeed shows that two independent correlations are observed for ^{1}H singlet and methyne carbons, corresponding to positions 4 and 4'. ^{1}H-^{1}H TOCSY clearly showed that protons at 5.79 and 5.82 ppm correlate with H3d, suggesting that these signals originate from the vinyl group from pyrrole D—H2d and H2d'. This further means that the doublet at 5.58 ppm comes from one of two CH_2 protons in pyrrole A (i.e., H2a), which is also implicated by NOESY and HSQC experiments. The triplet at 3.06 ppm and the signal at 2.51 ppm showed similar intensities and come from four protons in CH_2 groups in propionyl side chains. The peak of H7 protons is positioned downfield because of direct binding to carbonyl group. The most upfield shifted signals (in the range 2.02–2.27 ppm), show intensity of three protons each and were assigned to methyl groups. According to NOESY, signal at 2.27 ppm is from H1a protons that are close to H2a and H3a, i.e., pyrrole

Table 1 Chemical shifts and multiplicity of ^{1}H NMR peaks of biliverdin in DMSO

δ H (ppm)	Hydrogen type	Group	Multiplicity (J in Hz)
12.29	8	Propionyl carboxyl group	Broad
11.98 11.90	C B	Amino protons of pyrrolic rings	2 singlets
10.75 10.64	A D	Amino protons of lactam rings	2 singlets
7.58	5	Methyne bridge	Singlet
6.92	3d	CH non-equivalent methylene protons of vinyl groups	Doublet of doublets (18.38; 11.85)
6.69	3a	CH non-equivalent methylene protons of vinyl groups	Doublet of doublets (18.06; 11.61)
6.35	2a’	Vinyl group	Doublet (12.62)
6.32	4	Methyne bridge	Singlet
6.31	4’	Methyne bridge	Singlet
5.82 5.79	2d, 2d’	Vinyl group	Two doublets (10.87; 3.32)
5.58	2a	Vinyl group	Doublet (11.75)
3.06	7	Propionyl chain	Triplet (12.87)
2.51	6	Propionyl chain	Triplet (5.44)
2.27	1a	Methyl group	Singlet
2.19	1b	Methyl group	Singlet
2.16	1c	Methyl group	Singlet
2.02	1d	Methyl group	Singlet

A. Also, the spatial vicinity is observed between H2a’ and the proton with $\delta = 2.19$ ppm, which was attributed to H1b. The assignment of H4 and H4’ peaks was performed according to NOESY data: H4 (6.32 ppm) is connected with H1c (2.16 ppm) and H3d (6.92 ppm), whereas H4’ (6.31 ppm) is connected to both, H1a (2.27 ppm) and H1b (2.19 ppm).

NOESY delivered information on the conformation of BV in DMSO (Fig. 2). Probably, the most interesting result is that one carboxyl proton is placed in the vicinity of NH protons suggesting the bending of propionyl chain out of the plain toward central position of BV. The vicinity of H5 and H7 according to NOESY supported this hypothesis. NOE effect was significantly stronger for NH in one of the rings, most likely pyrrole C. This assignment is given by NOE effects between H1c and H4, and H1c and H7. H7 did not show detectable NOE effects for analogous protons in other three pyrrole rings (H1a, H1b, and H1d). It is noteworthy that this implies that the line at 11.98 ppm in ^{1}H NMR spectrum of BV comes from NH in pyrrole C (and $\delta = 11.90$ is from pyrrole B). NH in pyrrole C was closer to NH in pyrrole A or D than in other two rings. The latter is more probable taking into account the presence of NOE effect between H3d and H4 (H2d and H2d’ are probably pointed away from position 4), as well as H1c and H4. Therefore, in the ^{1}H NMR spectra, $\delta = 11.75$ ppm comes from NH in pyrrole A, whereas $\delta = 11.64$ is from pyrrole D. Protons on at least one of two H7 positions are close to H5. Cross peak intensities suggests that H2a’ is closer to H3a than H2a, whereas H3a is closer to H2a’ than H2a and H1a. Finally, the exchange peaks observed in the NOESY experiment between the pyrrole HN signals A-D and two minor peaks at 10.2 and 10 ppm suggest the presence of a minor species, probably due to a deprotonated form of BV present with a relative intensity of about 10%.

Biliverdin structure—simulations

Geometry and charge distributions of BV in DMSO were further established using UDFT. In addition, the structure of BV with all four protonated N atoms was compared to BV with an unprotonated N atom (Fig. S2). BV conformation with the lowest energy according to UDFT (Fig. 3) was in good agreement with NOESY data. The deprotonated and fully protonated BV structures are both stabilized by two intramolecular hydrogen bonds. The particularly strong one, with a length of ~2.0 Å is formed between bare nitrogen and hydrogen (from the -NH group) from the adjacent inner pyrrole ring (Fig. S2). The second hydrogen bond, formed between nitrogen and H from another terminal pyrrole ring, is significantly weaker, with a length of ~2.5 Å. The formation of these hydrogen bonds is in line with previous reports [5–9]. The protonation of N atom in pyrrole A alters BV conformation significantly (Fig. 3). Fully

Table 2 Connectivities observed, for each ^{1}H atom, in ^{1}H-^{13}C HSQC and ^{1}H-^{1}H TOCSY experiments for biliverdin in DMSO

Hydrogen type	δH (ppm)	HSQC δC (ppm)	TOCSY δH (ppm)
8	12.29		
C	11.98		
B	11.90		
A	10.75		
D	10.64		
5	7.58	119.36	
3d	6.92	126.67	2.02; 5.79
3a	6.69	126.67	5.58
2a’	6.35	122.10	2.27
4	6.32	95.09	
4’	6.31	95.47	
2d, 2d’	5.82 5.79	124.46	2.02; 6.92
2a	5.58	122.08	2.27; 6.69
7	3.05	20.19	
6	2.51	35.02	
1a	2.27	10.03	
1b	2.19	9.95	
1c	2.16	9.95	
1d	2.02	10.44	

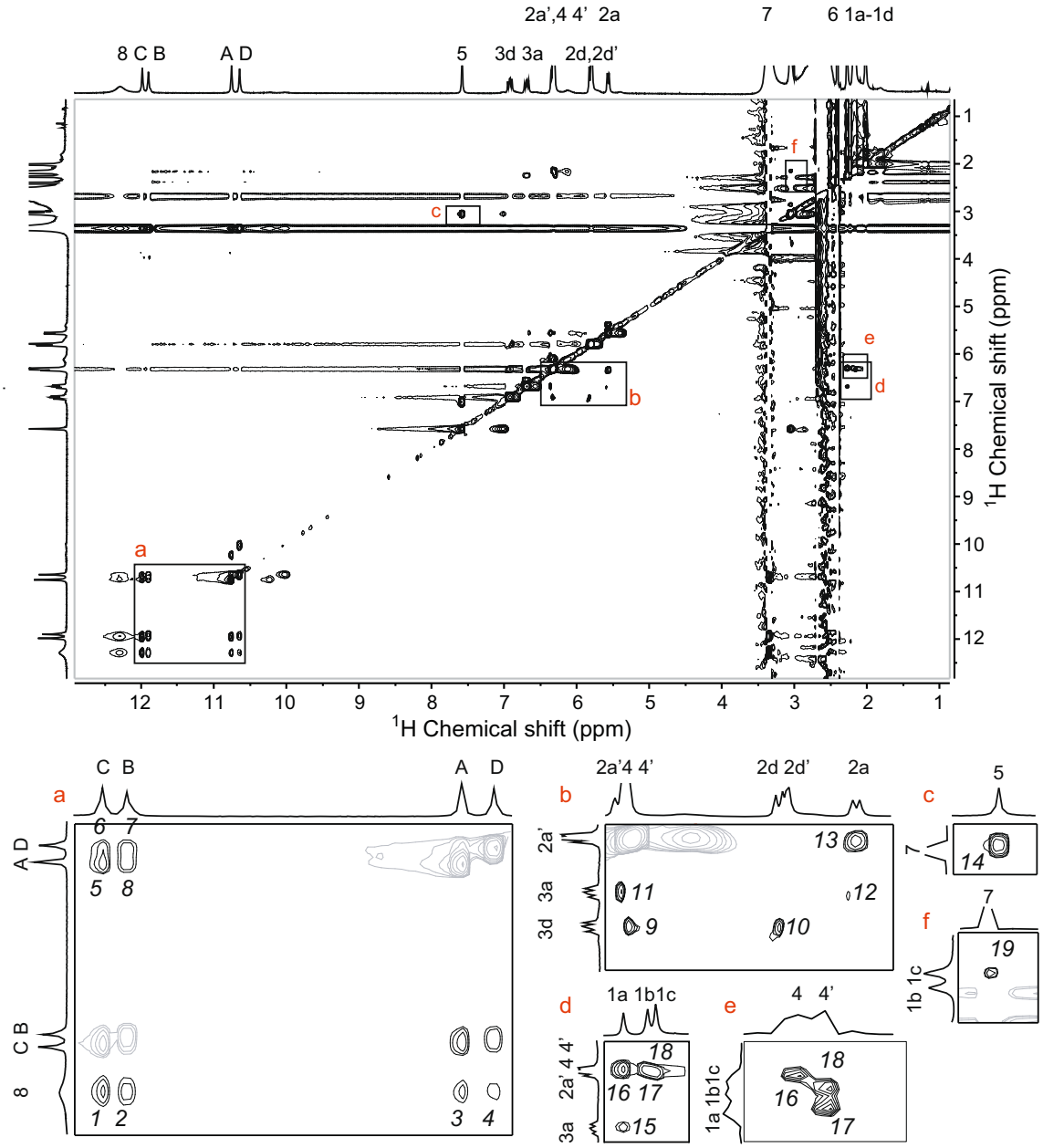

Fig. 2 500 MHz ^{1}H-^{1}H NOESY spectrum of biliverdin in DMSO. Cross-peaks of interest (1–19) are presented in separate panels (a–e) which represent different equally enlarged areas of the spectrum. Strong peaks (according to NOESY signal amplitude in arbitrary units) 10, 11, 13, 14, 16, 17, and 18; medium peaks 1, 5, 9, and 19; weak peaks 2, 3, 4, 6, 7, 8, 12, and 15

protonated BV is characterized by hydrogen bonds between hydrogen (from the -NH group) from one terminal pyrrole ring and carbonyl oxygen from the opposite terminal pyrrole ring. These bonds are enabled by a prominent out-of-plane bending of two terminal -NH groups with respect to pyrrole rings. The N–H bonds in the inner pyrrole rings are almost co-planar with those rings (dihedral angle between N-atom and adjacent C-atoms in terminal pyrroles is ~135°, whereas in the case of inner rings, it is ~160°, Fig. 3), and do not show hydrogen bonding. Also, torsions of pyrroles with respect to the CH groups (that connect pyrroles) are more pronounced for terminal rings. These two effects induce for -CO and -NH groups from the opposite terminal pyrrole rings to be directed one to another. These bonds are weaker than the strong H-bond in deprotonated BV, with lengths of ~2.25 and ~2.4 Å (Fig. 3). Simulations also showed bending of propionyl chain with carboxyl group out of the plain toward central position of BV. The down-field positions of A and C peaks compared to that of D and B in NMR spectra (Fig. 1), may be explained by the formation of a stronger hydrogen bond (for A), or closer proximity of carboxyl group (for C). The computed Mulliken charges are given

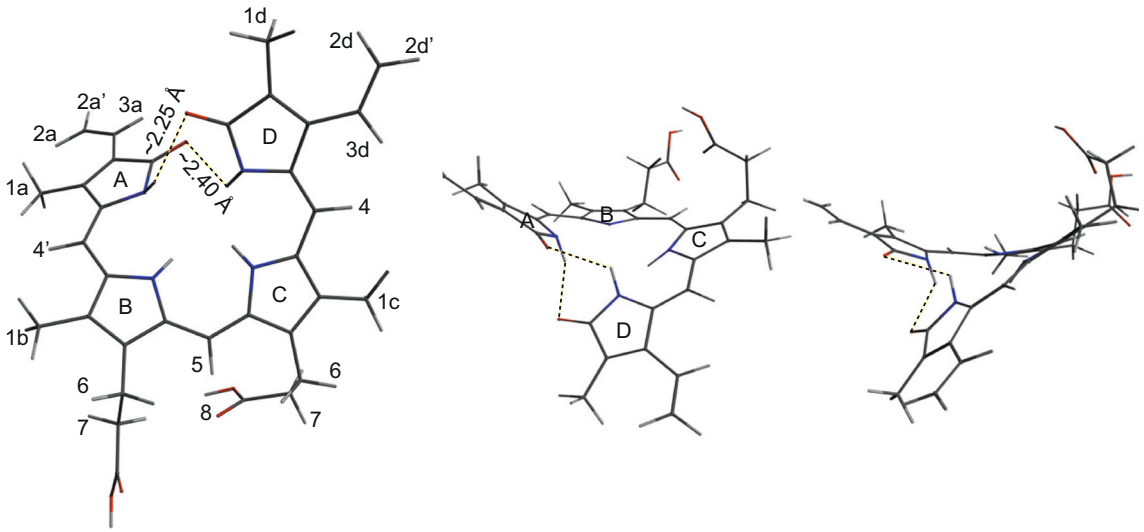

Fig. 3 3D structure derived from simulations (three different perspectives). The assigned protons/rings are labeled. Dashed lines are hydrogen bonds (calculated length is presented in Å)

in Fig. S3. According to the Mulliken charges, there is a significant charge redistribution upon protonation. The Mulliken charges of hydrogens are significantly affected, contrary to heavy elements that experience negligible changes. The inserted proton receives charge of about 0.65 e, resulting that all four atoms bonded to nitrogen become charged with ~+0.3 e. The charges of the other hydrogens decrease (in range from 0.01 to 0.08 e) maintaining the total +e charge of the molecule. This means that BV in DMSO is nominally BVH^+. It is important to stress out that the redistribution of charge and additional positive charge may impact the interactions with transition metals.

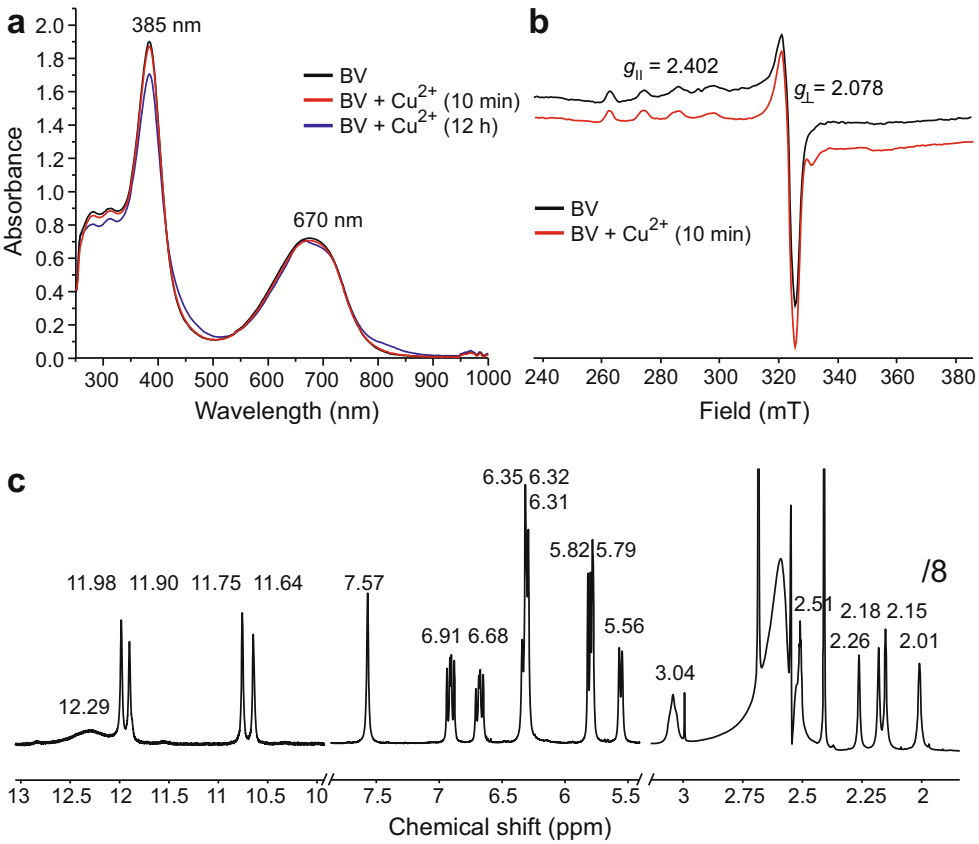

Fig. 4 The lack of coordinate interactions between biliverdin (BV) and Cu^{2+} in DMSO. **a** UV-Vis spectra of BV and BV/Cu^{2+} = 1 system. [BV] = 40 μM; pH = 4.5. **b** 110 K EPR spectra of Cu^{2+} (40 μM), in the absence and the presence of BV at equimolar concentration. **c** ^{1}H NMR spectrum of BV in the presence of Cu^{2+} at equimolar concentration in DMSO at 298 K. The pH of the solution ([BV] = 2 mM) was ~4. The vertical intensity of the 3–2 ppm region is divided by a factor 8

The lack of coordinate interactions of biliverdin with Cu^{2+}

UV-Vis spectrum of BV in DMSO was not affected by Cu^{2+} at equimolar concentration, even after prolonged incubation under aerobic conditions (Fig. 4a), implying that BV and Cu^{2+} do not build a complex in DMSO. This was further confirmed by low-T EPR spectra of Cu^{2+} and ^{1}H NMR spectra of BV, which remained practically unaltered in the presence of BV or Cu^{2+}, respectively (Fig. 4b, c). It is noteworthy that Cu^{2+} exhibited an anisotropic EPR signal in DMSO, with a strong $g_{\perp} = 2.078$ line, and four weak lines coming from hyperfine coupling with $^{63}Cu/^{65}Cu$ nuclei ($I = 3/2$, $S = 1/2$) along $g_{\parallel} = \sim 2.402$ (Fig. 4b). The g values ($g_{\parallel} > g_{\perp} > g_e$ (g value for free electron = 2.0023)), and the spectral shape imply that Cu^{2+} in DMSO is in octahedral coordination environment with tetragonal distortion [28, 29]. This is in line with previous studies showing that Cu^{2+} builds coordination complexes with DMSO and Cl^{-} ions, such as $Cu(DMSO)_3Cl^{+}$, $Cu(DMSO)Cl_3^{-}$, and $Cu(DMSO)_2Cl_2$ [30, 31]. The coordination of Cu^{2+} by the solvent may (at least partially) be responsible for the lack of formation of BV–Cu^{2+} complex in DMSO. On the other hand, the peaks of all four protons on N atoms could be observed in the ^{1}H NMR signal of BV in the presence of Cu^{2+} (Fig. 4c). This confirmed the previously proposed inability of Cu^{2+} to replace the NH protons in BV in this solvent [11].

Taking into account that deprotonation represents a critical step in coordinate bonds' formation, it may represent a key difference between the interactions of BV with copper in different solvents. BV contains an unprotonated N in solvents that "allow" the formation of BV-Cu complex - water and in chloroform [5, 7, 22]. In DMSO, all four protonated N atoms, as well as additional positive charge and altered charge redistribution, may hinder cooperation in the formation of multiple coordinate bonds [32, 33]. It is noteworthy that "elusive" effects of DMSO in buffered mixtures with water on experimental measurements of *pK* values of tetrapyrroles represent a long-standing question of biochemistry [8, 34]. Pertinent to this, we have noted that even small amounts of water in DMSO may significantly alter the interactions of BV and Cu^{2+} [5]. It appears that a caution has to be exerted to prevent artifacts that may be induced by traces of water in DMSO. Finally, it is worth mentioning that BV and its derivative—bilirubin, do not share the same sensitivity to solvents. It has been proposed that bilirubin maintains conformation which is stabilized by intramolecular hydrogen bonds between carboxyl groups and -NH and -CO groups in pyrroles, across a variety of solvents—DMSO, chloroform, and phosphate buffer [35]. The instability of conformation of BV, in different environments and the potential presence of two forms of BV—deprotonated and protonated cationic, may be one of the "reasons" for the investment of two electrons form NADPH into reduction of BV to more "predictable" bilirubin [4].

Conclusions

The key features of BV conformation in DMSO are as follows: (i) protonation of all four N atoms, (ii) hydrogen bonds between hydrogen (from -NH group) from one terminal pyrrole ring and carbonyl oxygen from the opposite terminal pyrrole ring, (iii) bending of propionyl chain out of the plain toward central position of BV, and (iv) additional positive charge and altered charge redistribution. This may hinder cooperation in the formation of multiple coordinate bonds and the formation of complex with copper. The presented results may shed a new light on the importance of protonation, hydrogen bonds, and solvents in coordination chemistry.

Acknowledgments We are thankful to Prof. Miloš Mojović at EPR Laboratory, Faculty of Physical Chemistry, University of Belgrade for recording EPR spectra and to Ljiljana Stojanović from School of Biological and Chemical Sciences, Queen Mary University of London, for her great help in calculating and discussing theoretical results obtained using the UDFT.

Funding information This work was supported by the Ministry of Education, Science and Technological Development of the Republic of Serbia (III43010). This article is based upon work from COST Action CA15133 FesBioNet, supported by COST (European Cooperation in Science and Technology).

Compliance with ethical standards

Conflict of interest The authors declare that they have no conflict of interest.

References

1. Korać J, Todorović N, Zakrzewska J, Žižić M, Spasojević I (2018) The conformation of epinephrine in polar solvents: an NMR study. Struct Chem 29:1533–1541
2. Watermann T, Elgabarty H, Sebastiani D (2014) Phycocyanobilin in solution - a solvent triggered molecular switch. Phys Chem Chem Phys 16:6146–6152
3. Sailofsky BM, Brown GR (1987) Solvent effects on the photoisomerization of bilirubin. J Chem 65:1908–1916
4. Nam J, Lee Y, Yang Y, Jeong S, Kim W, Yoo JW, Moon JO, Lee C, Chung HY, Kim MS, Jon S, Jung Y (2018) Is it worth expending energy to convert biliverdin into bilirubin? Free Radic Biol Med 124: 232–240
5. Dimitrijevic MS, Bogdanović Pristov J, Žižić M, Stanković DM, Bajuk-Bogdanović D, Stanić M, Spasić S, Hagen W, Spasojević I (2019) Biliverdin-copper complex at physiological pH. Dalton Trans. https://doi.org/10.1039/c8dt04724c
6. Krois D, Lehner H (1993) Helically fixed chiral bilirubins and biliverdins: a new insight into the conformational, associative and dynamic features of linear tetrapyrrols. J Chem Soc Perkin Trans 2: 1351–1360
7. Lightner DA, Holmes DL, McDonagh AF (1996) On the acid dissociation constants of bilirubin and biliverdin. pKa values from 13C NMR spectroscopy. J Biol Chem 271:2397–2405
8. Lightner DA, Holmes DL, McDonagh AF (1996) Dissociation constants of water-insoluble carboxylic acids by 13C-NMR. pKas of

mesobiliverdin-XIIIα and mesobilirubin-XIIIα. Experientia 52: 639–642
9. Sugishima M, Sakamoto H, Higashimoto Y, Noguchi M, Fukuyama K (2003) Crystal structure of rat heme oxygenase-1 in complex with biliverdin-iron chelate. Conformational change of the distal helix during the heme cleavage reaction. J Biol Chem 278:32352–32358
10. Reichardt C (2003) Solvents and solvent effects in organic chemistry. Wiley-VCH Verlag GmbH & Co, Weinheim
11. Sóvágó I, Harman B, Kolozsvári I, Matyuska F (1985) Complex-formation and redox reactions of bilirubin and biliverdin with zinc(II), cadmium(II) and copper(II) ions. Inorg Chim Acta 106: 181–186
12. Berlec A, Štrukelj B (2014) A high-throughput biliverdin assay using infrared fluorescence. J Vet Diagn Investig 26:521–526
13. Shang L, Rockwell NC, Martin SS, Lagarias JC (2010) Biliverdin amides reveal roles for propionate side chains in Bilin reductase recognition and in holophytochrome assembly and photoconversion. Biochemistry 49:6070–6082
14. Mukerjee P, Ostrow JD (1998) Effects of added dimethylsulfoxide on pKa values of uncharged organic acids and pH values of aqueous buffers. Tetrahedron Lett 39:423–426
15. McDonagh AF, Phimster A, Boiadjiev SE, Lightner DA (1999) Dissociation constants of carboxylic acids by 13C-NMR in DMSO/water. Tetrahedron Lett 40:8515–8518
16. Rubino JT, Berryhill WS (1986) Effects of solvent polarity on the acid dissociation constants of benzoic acids. J Pharm Sci 75:182–186
17. Kurtin WE, Enz J, Dunsmoor C, Evans N, Lightner DA (2000) Acid dissociation constants of bilirubin and related carboxylic acid compounds in bile salt solutions. Arch Biochem Biophys 381:83–91
18. Ostrow JD, Celic L, Mukerjee P (1988) Molecular and micellar associations in the pH-dependent stable and metastable dissolution of unconjugated bilirubin by bile salts. J Lipid Res 29:335–348
19. Li M, Xiao Z, Xiang H, Lu Z (1997) Unusual solvent effect on absorption spectra of nonplanar dodecaphenylporphyrins with different substituents. Spectrochim Acta A Mol Biomol Spectrosc 53: 1691–1695
20. Moussa F, Kanoute G, Herrenknecht C, Levillain P, Trivin F (1988) Electrochemical oxidation of bilirubin and biliverdin in dimethyl sulfoxide. Anal Chem 60:1179–1185
21. Lu G, Lin W, Fang Y, Zhu W, Ji X, Ou Z (2011) Synthesis and electrochemical properties of meso-phenyl substituted copper corroles. Solvent effect on copper oxidation state. J Porphyrins Phthalocyanines 15:1265–1274
22. Balch AL, Mazzanti M, Noll BC, Olmstead MM (1993) Geometric and electronic structure and dioxygen sensitivity of the copper complex of octaethylbilindione, a biliverdin analog. J Am Chem Soc 115:12206–12207
23. Dorazio SJ, Halepas S, Bruhn T, Fleming KM, Zeller M, Brückner C (2015) Singlet oxygen oxidation products of biliverdin IXa dimethyl ester. Bioorg Med Chem 23:7671–7675
24. Feliz M, Ribó JM, Salgado A, Trull FR, Vallès MA (1989) On the 1H NMR spectra of biliverdins with free propionic acid substituents. Mönatsh Chem 120:445–451
25. Kaplan D, Navon G (1982) Studies of the conformation of bilirubin and its dimethyl ester in dimethyl sulphoxide solutions by nuclear magnetic resonance. Biochem J 201:605–613
26. Pretsch E, Bühlmann P, Badertscher M (2009) Structure determination of organic compounds. Springer-Verlag, Berlin
27. Bates RG (1973) Determination of pH: theory and practice. Wiley & Sons, New York
28. Hathaway BJ, Billing DE (1970) The electronic properties and stereochemistry of mono-nuclear complexes of the copper(II) ion. Coord Chem Rev 5:143–207
29. Garribba E, Micera G (2006) The determination of the geometry of Cu(II) complexes. J Chem Educ 83:1229–1232
30. Elleb M, Meullemeestre J, Schwing-Weill MJ, Vierling F (1982) Spectrophotometric study of copper(II) chloride complexes in propylene carbonate and in dimethyl sulfoxide. Inorg Chem 21:1477–1483
31. Willett RD, Chang K (1970) The crystal structure of copper(II) chloride bis(dimethylsulphoxide). Inorg Chim Acta 4:447–451
32. Kozlowski H, Kowalik-Jankowska T, Jeżowska-Bojczuk M (2005) Chemical and biological aspects of Cu2+ interactions with peptides and aminoglycosides. Coord Chem Rev 249:2323–2334
33. Meng R, Becker J, Lin FT, Saxena S, Weber SG (2005) Binding of copper(II) to thyrotropin-releasing hormone (TRH) and its analogs. Inorg Chim Acta 358:2933–2942
34. Mukerjee P, Ostrow JD, Tiribelli C (2002) Low solubility of unconjugated bilirubin in dimethylsulfoxide–water systems: implications for pKa determinations. BMC Biochem 3:17
35. Nogales D, Lightner DA (1995) On the structure of bilirubin in solution. J Biol Chem 270:73–77